Lab on a Chip

On-chip organic synthesis enabled by engine-and-cargo in an electrowetting-on-dielectric digital microfluidic device

Journal:	*Lab on a Chip*
Manuscript ID	LC-ART-05-2019-000428.R2
Article Type:	Paper
Date Submitted by the Author:	25-Jul-2019
Complete List of Authors:	Torabinia, Matin; University of Texas at Arlington, Mechanical and Aerospace Engineering Asgari, Parham; University of Texas at Arlington, Chemistry and Biochemistry Dakarapu, Udaya sree; University of Texas at Arlington, Chemistry and Biochemistry Jeon, Junha; University of Texas at Arlington, Department of Chemistry and Biochemistry Moon, Hyejin; University of Texas at Arlington, Mechanical and Aerospace Engineering

On-chip organic synthesis enabled by engine-and-cargo in an electrowetting-on-dielectric digital microfluidic device

Matin Torabinia[1], Parham Asgari[2], Udaya Sree Dakarapu[2], Junha Jeon[2], and Hyejin Moon[1]
[1]Mechanical and Aerospace Engineering, The University of Texas at Arlington
[2]Chemistry and Biochemistry, The University of Texas at Arlington

This paper presents the microfluidic chemical reaction using an electrowetting-on-dielectric (EWOD) digital microfluidic device. Despite of numbers of chemical/biological applications using EWOD digital microfluidic device, its application to organic reactions have been seriously limited because most of common solvents used for synthetic organic chemistry are not operable on EWOD device. To address this unsolved issue, we first introduce a novel technique of an "engine-and-cargo" system that enables use of non-movable fluids (e.g., organic solvents) on an EWOD device. With esterification as the model reaction, on-chip chemical reactions were successfully demonstrated. Conversion data obtained from on-chip reactions were used in the demonstration of reaction characterization and optimization such as reaction kinetics, solvent screening, and catalyst loading. As the first step toward on-chip combinatorial synthesis, parallel esterification of three different alcohols were demonstrated. Results from this study clearly show that EWOD digital microfluidic platform is a promising candidate for a microscale chemical reaction.

1. Introduction

Over the past decades, microscale chemical reaction technology has been attractive in diverse areas of chemistry.[1-3] It allows the precise control of quantified reagents and highly efficient heat and mass transfer, because of a large interface-to-volume ratio–particularly in case of the exothermic reaction and mixing–, reduced consumption of toxic or expensive agents, improved reaction profiles, and enhanced selectivity compared to macro-scale reactions.[4-6]

The mainstream microscale reaction processes were established using continuous microchannel flow systems. Lob et al.[7] performed fluorination of toluene in microchannel reactors made of silicon. Miller et al.[8] showed rapid formation of amides via carbonylative cross-coupling of aryl halides with benzyl amine using a reaction channel. Both cases achieved the higher yields than conventional batch reactions within the same time periods. Other examples include Suzuki cross-coupling,[9] Wittig olefination reaction,[10] nitration of benzene, and tripeptide synthesis.[11] Despite of successful demonstration from prior studies, microchannel-based approaches suffer from several limitations. For example, clogging of the channels by products or byproducts may cause the difficulty of maintaining a constant hydrodynamic pressure, thus stable flow.[4] Requirement of complex flow network and cross-contamination due to unwanted diffusion through channels are also concerned. Moreover, solvent-swapping processes pose very challenging problems in microchannel reactors. Another drawback of microchannel reactors presents in combinatorial chemistry–a powerful tool for lead compound discovery and optimization of new drugs and materials.[12] Since a combinatorial synthesis through either batch or flow reactors requires as many reactors as the number of all possible combinations of reactants, the reactor system tends to be excessively complex.

A digital microfluidic platform using electrowetting-on-dielectric (EWOD) principle can be an alternative and/or complement a microchannel reactor. An EWOD digital microfluidic platform eliminates the necessity of predetermined channel network and mechanical pumps and valves. Since it is a droplet-based flow, it can prevent cross-mixing and cross-contamination. Each droplet plays as a batch reactor, which brings the feasibility of performing multi-step reactions that may involve with solvents swapping and combinatorial synthesis.[13-15] Researchers have taken advantages of these unique features of EWOD microfluidic devices to conduct on-chip chemical

reactions, e.g. reactions in ionic liquid droplets,[16] synthesis of radiotracers,[17] and synchronized synthesis of peptide-based macrocycles.[18] Of note, that all these reactions on EWOD chip mentioned above utilized solvent fluids that are movable by EWOD actuation. However, contemporary organic synthesis generally requires non-polar or polar aprotic solvents, and their poor movability in an EWOD chip has been a long-standing problem.

Chatterjee et al.[19] experimentally assessed the movability of organic solvents and solutions in the EWOD system. In this study, many organic solvents such as cyclohexane, carbon tetrachloride, chloroform, and toluene cannot be displaced by EWOD actuations. Recently, Torabinia et al.[20] reported an electromechanical model that can predict the movability of a fluid by an EWOD device. This study showed that both the magnitude and the frequency of the operation voltage need to be tuned to obtain maximum force in an EWOD device. At the particular experimental parameters, their model predicted that many indispensable organic solvents for organic synthesis are not movable, which concurs with the results by Chatterjee et al.

Nevertheless, a couple of efforts were made to operate non-movable fluids in EWOD device. Inspired by Brassard et al.[21], Li et al.[22] demonstrated manipulations of oil, organic, and gaseous chemicals in the aqueous shell. However, such configuration fails to host fluids having a lower surface tension than aqueous solutions. For instance, most of organic solvents have much lower surface tensions (~ 20 mN/m) than that of water, which does not allow them to be encapsulated in an aqueous shell. In addition, additional capillary tube settings were needed to create core-shell droplets, leading to unfavorable complexities of device design and fabrications. Another approach was to use dielectrophoretic (DEP) force to operate non-movable fluids; Fan et al.[23] reported the manipulation of a silicone oil droplet by DEP force in a typical EWOD device. However, exerting DEP force required extremely higher voltage than the EWOD operation does. In addition, fluids must have some specific dielectric properties to be manipulated by DEP force. In fact, according to Torabinia et. al.[20], most of essential organic solvents for chemical reactions are not movable, even in the range of frequency at which DEP force is dominant. These hindrances limit the scope of possible chemical reactions in an EWOD device.

As addressing abovementioned challenges, this paper introduces a new strategy of *"engine-and-cargo"* which enables an EWOD device to handle electrically non-responsive fluids such as

organic solvents. This approach can allow to host a wide range of organic syntheses in EWOD devices. It has long been suggested that the true product from microfluidic reaction systems would be information, rather than a more tangible substances or intermediates.[4, 24] As like other types of microfluidic reactors, on-chip syntheses in EWOD devices would transform to parallel reactor systems (i.e., numbering up) rather than to scale up to production systems. Vast information obtained from fast and automated on-chip chemical reactions would be primarily utilized for reaction optimization and chemical discovery. Especially, when EWOD devices are capable of integrating on-chip chemical synthesis capacity with biological/biomedical functions such as cell culture,[25] bio-separations,[26, 27] and biosensors,[28] this ideally permits to build a complete drug discovery platform.

In this study, we chose esterification as a model reaction to demonstrate the capability of an EWOD device which can perform on-chip organic synthesis. Using conversion data obtained from on-chip reactions, characterization and optimization of the reactions were conducted. To confirm the soundness of on-chip data, same reactions were conducted in lab-scale. In addition, as the first step toward on-chip combinatorial synthesis, parallel esterification reactions of three different types of alcohols were established.

2. Problem Description

2.1 Engine-and-cargo system

An engine-and-cargo system harnesses a compound droplet of two immiscible liquids. An engine refers to the liquid that has the electrowetting properties; a cargo is the other one without electrowetting properties, thus non-movable in an EWOD device.

Figure 1 shows the formation and operation of an engine-and-cargo system in an EWOD device. In this example, ionic liquid ([bmim]PF_6) works as the engine and toluene is carried as the cargo. As shown in Fig. 1(a), the ionic liquid has electrowetting properties so that it moves as responding to the applied voltage on electrodes underneath it, whereas toluene stays unresponsive under any magnitude and frequency of voltages.[19] When the ionic liquid droplet approaches to the toluene droplet, it is encapsulated by toluene spontaneously to minimize the surface free energy and forms a compound droplet (Fig. 1(b)). Note that surface tension of ionic liquid (~ 40 mN/m) is higher

than that of toluene (~ 20 mN/m). Figure 1(c) presents the motion of the engine-and-cargo system, arising from the electrowetting force exerted on the engine that carries the cargo by viscous drag force. Evidently, the designed engine-and-cargo system enables the use of toluene and other non-movable liquids in a typical EWOD device without any modification of device structures and architectures. In the later section of this study, it is reported that all the basic fluidic functions of an EWOD digital microfluidic device including dispensing, transporting, merging, and splitting of droplets are achieved with electrically non-responsive fluids. This technique has the potential to make substantial advances on biological and chemical protocols processed on EWOD digital microfluidic device.

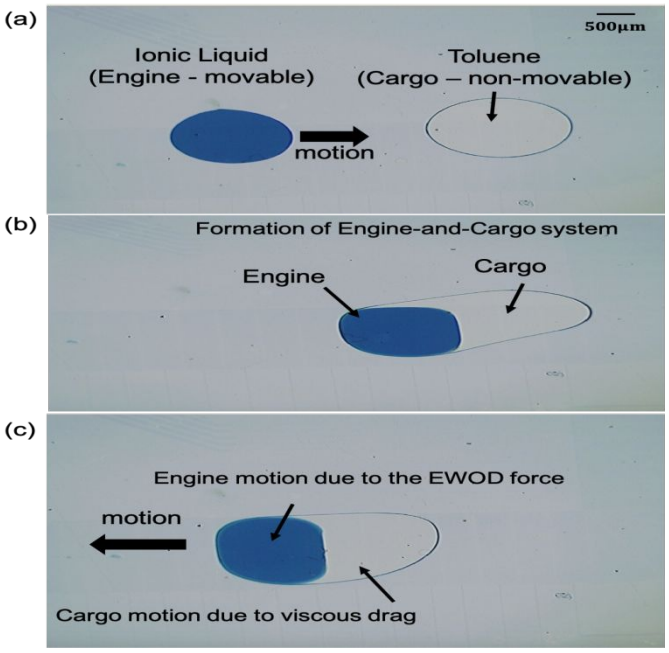

Fig. 1 The formation of the engine-and-cargo system of an ionic liquid([bmim]PF_6) as the engine (movable) and toluene as the cargo (non-movable). (a) Actuation of the engine towards the cargo, (b) encapsulation and formation of engine-and-cargo, and (c) the motion of an engine droplet by electrowetting operation leads motion of an entire compound droplet, thus fluidic functionalities of cargo droplet. Images from the top view of the EWOD device. Blue dye was added to the ionic liquid for the better visualization purpose only.

2.2 Esterification Reaction

Esters are one of the important classes of organic molecules that are widely used in synthesis of fine chemicals, drugs, food preservatives, perfumes, plasticizers, and pharmaceuticals.[29-31] In a

biological aspect, acetylation is one of important protein modification methods in cell biology that has an impact on gene expression and metabolism.[32] There are high demands of rapid, simple, and environmentally friendly protocols for the microscale esterification of alcohols for facile production of a wide variety of esters for medicinal and biological applications.[33-35] Hence, the esterification in microchannel reactors has been studied comprehensively.[24, 36-40]

In this study, we chose esterification of alcohols with acetic anhydride as our model reaction to demonstrate the on-chip organic synthesis capabilities of an EWOD digital microfluidic device. Total 60 tests of 20 different conditions of esterification reactions of secondary alcohols with acetic anhydride were carried out on-chip. The esterification of menthol is shown in Fig. 2. A traditional macroscale esterification (e.g., flask-based protocol) involves aliquoting, introducing, and mixing reagents, followed by quenching the reaction at controlled time. Instead, on EWOD chip, a reaction can be initiated by generating reagents droplets, transporting, and merging droplets, and at the end of the processes the reaction is quenched by merging the reacting droplet with the quenching agent droplet.

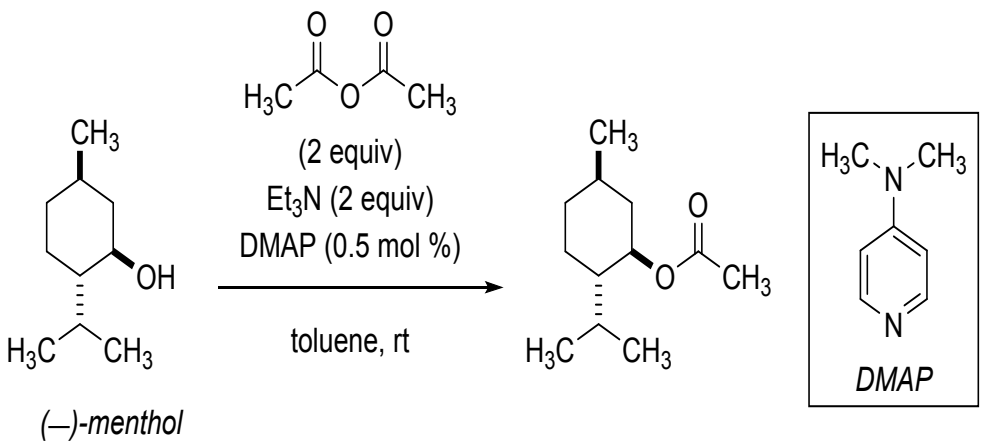

Fig. 2 Model esterification reaction using menthol, acetic anhydride (Ac2O), trimethylamine (Et3N), and DMAP in the presence of specific solvent.

3. Experiment

3.1 Device fabrication and experimental setup

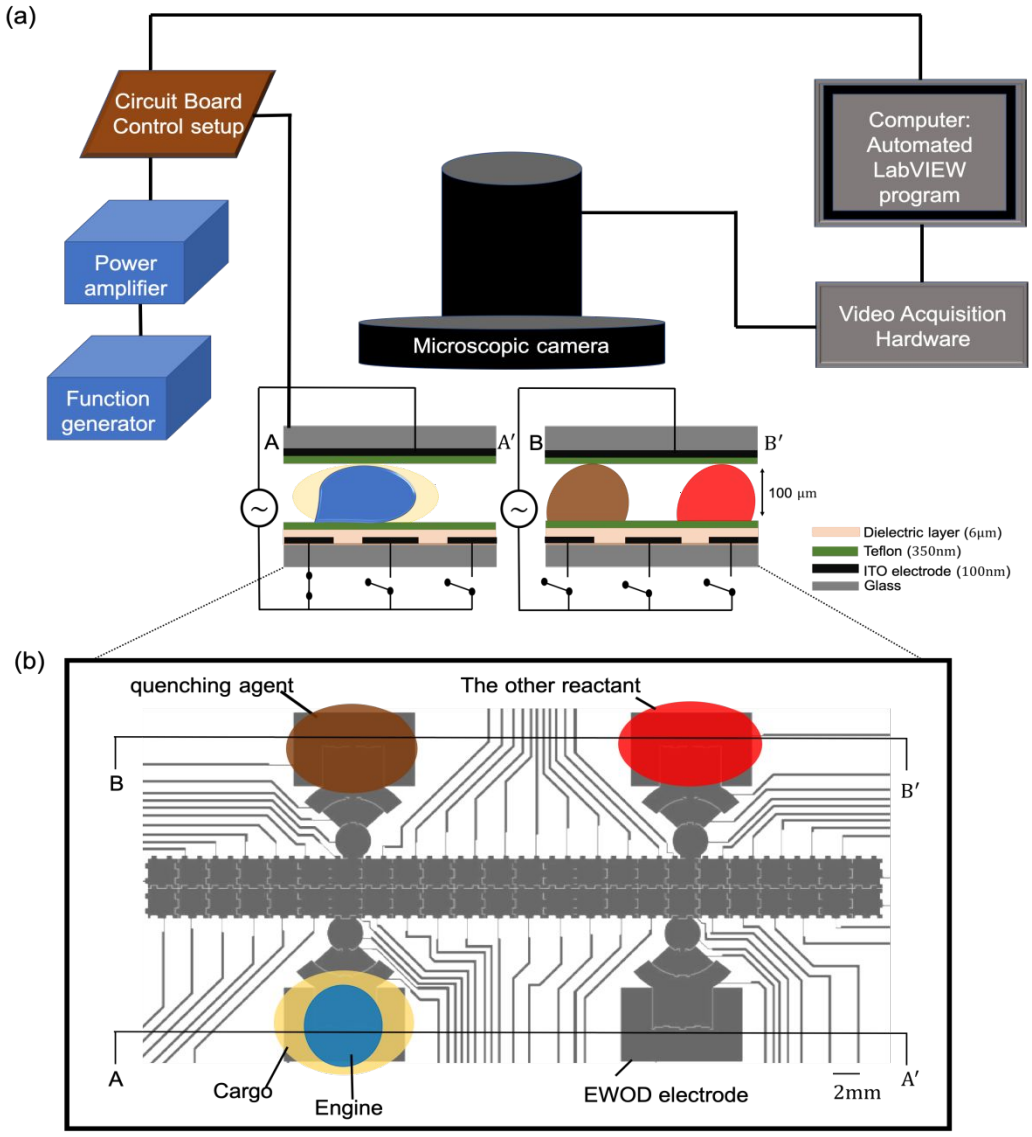

Fig. 3 (a) The experimental setup and the side view schematics of the EWOD chip operation, and (b) The EWOD chip electrodes layout and the placement of reagents on the chip at the beginning of each test. The cargo is the solution of a part of reactants and the catalyst - menthol, trimethylamine, and DMAP. The other reactant is acetic anhydride solution. The engine is [bmim]PF6. The quenching agent is saturated aqueous sodium bicarbonate. The surrounding medium is air throughout all the experiment.

All EWOD microfluidic devices used in this study were fabricated in the Shimadzu Institute Nanotechnology Research Center of the University of Texas at Arlington. Actuation electrodes in the bottom plate of an EWOD device were fabricated by photolithography followed by wet etching of an indium tin oxide (ITO) layer (100 nm) coated on a glass wafer. The dielectric layer (SU-8, 5μm) and the hydrophobic layer (Teflon, 300 nm) were spin-coated and oven baked. The details of the fabrication steps can be found elsewhere [20, 41] and in ESI.

The EWOD operation voltages (100 Vrms at 1 kHz) were provided by Agilent arbitrary waveform generator and the TEGAM high voltage amplifier (model 23400). Desired sequence of turning on/off electrodes were applied through LabVIEW program. Droplet motions were recorded using Hirox KH-1300 digital microscope system.

3.2 Materials

(–)-Menthol (99%), phenol, ≥99.5% (GC), Benzyl alcohol anhydrous, 99.8%, trimethylamine, acetic anhydride, 4-(dimethylamino) pyridine (DMAP) (≥ 90%) were purchased from SIGMA-ALDRICH (USA). Toluene (Certified ACS), 1,4-dioxane, N,N-dimethylformamide, 1,1-dichloroethane (DCE), dichloromethane, (>99.8%) and 1-butyl-3-methylimidazolium hexafluorophosphate ([bmim]PF_6) (98+%) obtained from Fisher Scientific. Assorted food and egg dye purchased form Walmart (USA). All chemicals were analytical grade and used as received.

Before each test, reagents were placed in designated reservoirs as illustrated in Fig. 3(b). Among the esterification reagents listed in Fig. 2, alcohol (i.e., menthol), trimethylamine, and DMAP were identified as non-movable fluids on the EWOD platform. Alcohol (5 μmol), trimethylamine (10 μmol), and DMAP (0.1 to 5 mol %) were separately prepared with the same solvent of interest and mixed by the same volume. Then the mixed solution was placed at the ‘cargo’ reservoir, where they were sitting together with the ‘engine’ fluid (i.e., ionic liquid). On the other hand, acetic anhydride (acylating reactant, 10 μmol) and sodium bicarbonate (quenching agent) are movable in the EWOD platform due to their electrowetting properties, so that they were operated without the help of engine droplets.

3.3 Test Protocols

Both lab-scale and on-chip reactions were carried out to compare their conversion at each reaction condition. The detail of lab-scale esterification reaction protocol can be found in ESI. Following sections describe the detail of the on-chip reaction protocol.

3.3.1 Formation of an engine-and-cargo droplet

Each test began with forming an engine-and-cargo compound droplet. Figure 4 shows the sequence of formation of an engine-and-cargo droplet from the reservoir. First, EWOD forces let an engine liquid droplet dispensed from its reservoir puddle (Fig. 4(a)-(b)) while the cargo puddles remained non-responsive to the sequence of activation voltages. As the engine droplet was dispensed and moved further away from the reservoir, cargo solution was drawn together due to the viscous drag force between the engine droplet and the cargo solution and a neck in the cargo solution formed (Fig. 4(c)). Afterwards, the hydrodynamic instability at the cargo neck eventually let it pinch-off as shown in Fig. 4(c) and (d). The completely detached droplet from the reservoir was an engine-and-cargo compound droplet (Fig. 4(d)).

The volume of dispensed cargo solution was estimated by multiplying the footprint area (i.e., the area observed from the top view of the droplet) of cargo with the gap between top and bottom plates of the device. Note that the gap (= 100 μm) was well controlled and kept invariant throughout the entire device, so the variation in the footprint are was directly proportion to the variation in the droplet volume. The footprint area of cargo was measured using ImageJ software. The details of the volume measurement and calibration is described in ESI.

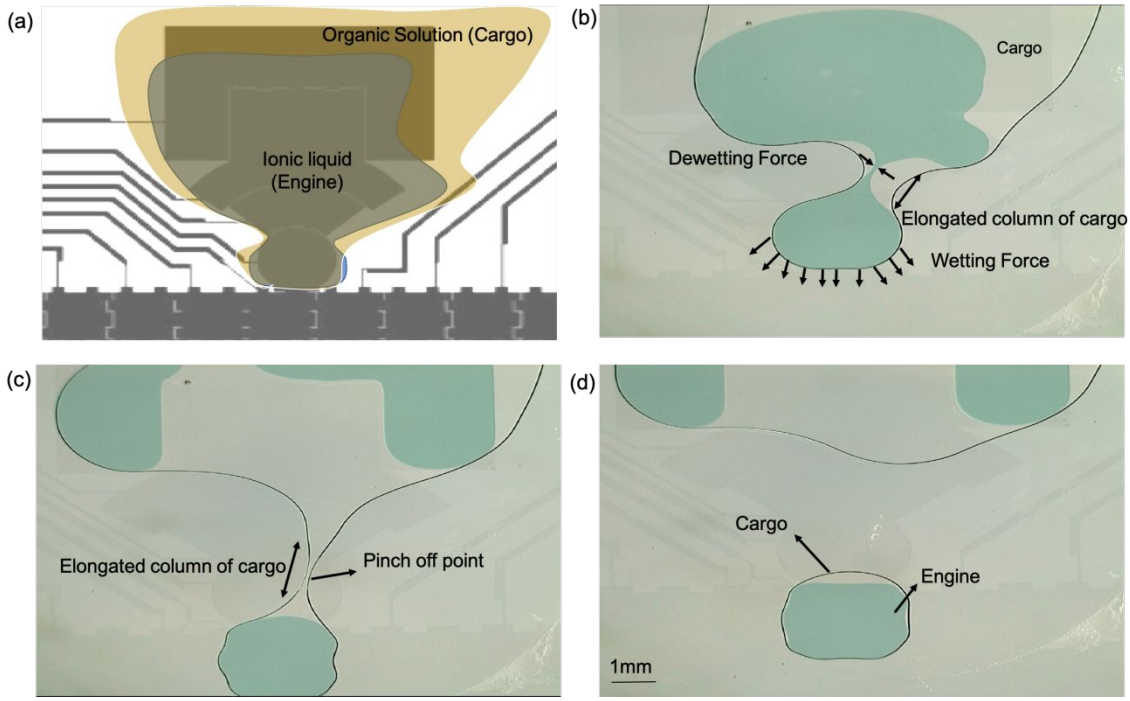

Fig. 4 A sequence of formation of an engine-and-cargo compound droplet from the reservoir. (a)The initial state, (b) The viscous drag between the engine and cargo fluids stretched the cargo fluid, (c) The engine droplet was dispensed and it pulled the cargo further so that a neck formed in the cargo and the hydrodynamic instability grew, and (d) the cargo neck eventually pinched off and formed an engine-and-cargo. The snapshot in (a) was image processed to clearly present the electrodes layout while it shows the beginning of the dispensing process.

3.3.2 On-chip reactions

Figures 5(a)-(f) summarize the general procedure of each on-chip reaction test protocol. First, an engine-and-cargo was dispensed (Fig. 5(a)). Then, a droplet of the other reactant solution was dispensed from its reservoir and it was merged with the previously dispensed engine-and-cargo (Fig. 5(b)). As they merged, the esterification began and continued to proceed (Fig. 5(c)). A droplet of a quenching agent was dispensed from the reservoir and delivered to the reacting droplet at the prescribed reaction time (Fig. 5(d)). This let the reaction stop right at the prescribed reaction time (Fig. 5(e)). Then, the reaction mixture (organic layer) was carefully drawn out using a syringe and diluted with DCM in a GC vial, which was subjected to the GC-MS analysis to measure a conversion of the reaction (Fig. 5(f)).

While demonstrating capability of an EWOD device to carry out organic reactions, three reaction parameters–reaction time, type of solvents, and catalyst concentration–of on-chip esterification reactions of secondary alcohols with acetic anhydride were independently evaluated and summarized in Fig. 5(g).

For the kinetic study, other reaction parameters (e.g., catalyst concentration and solvent) were fixed and the reaction were monitored from 10 s to 90 s. For the solvent screening, catalyst concentration and reaction time were fixed and 4 different solvents (i.e., toluene, dioxane, N,N-dimethylformamide, and DCE) were tested. For the optimization of catalyst loading, solvent and reaction time were fixed and the concentration of catalyst was varied from 0.1 to 1.5 mol %.

As simulating parallel synthesis, we performed esterification of three substrates including menthol, benzyl alcohol, and phenol with acid anhydride under basic conditions (Fig. 5(g), the bottom row) on a single EWOD chip. In the beginning of the test, all reagents including 3 substrates were placed in the designated reservoirs of the chip. To be able to perform true parallel reactions (i.e., 3 reactions run simultaneously), complete automation of EWOD chip operation is necessary. Because the scope of this study did not include full automation of the device, 3 reactions were performed in series as each reaction followed the order of Fig. 5(a)-(f). However, this does not limit the capability of an EWOD device to host parallel or combinatorial synthesis. The reactivity difference of these three substrates was examined over the first 30 s of each reaction.

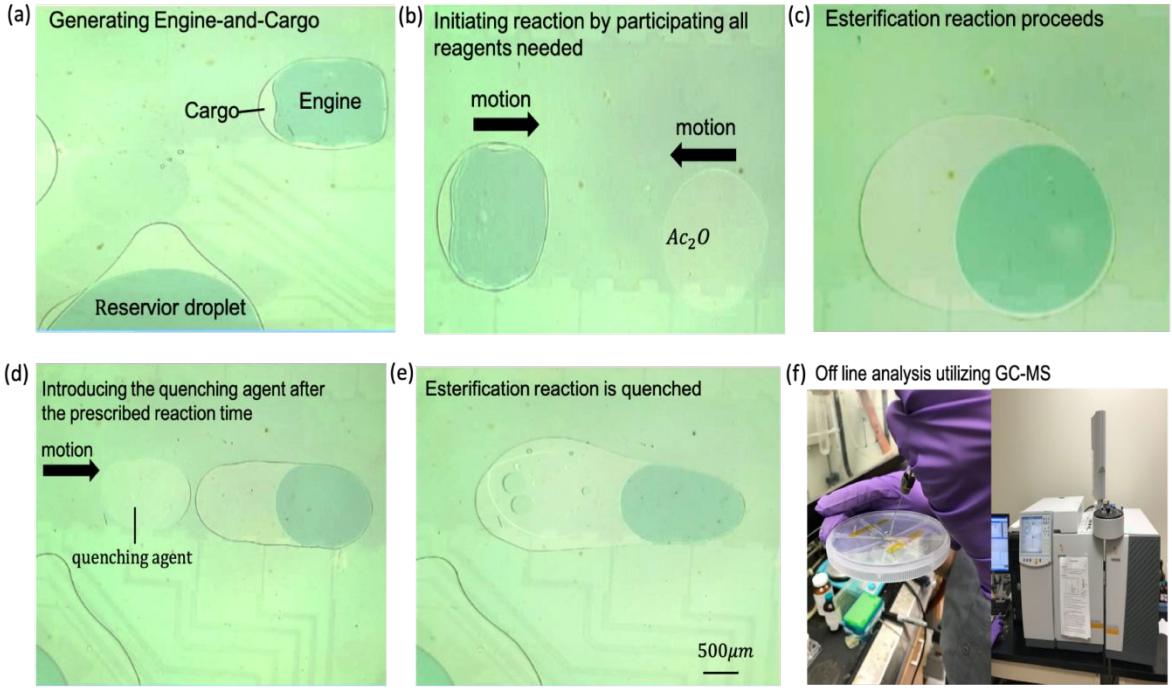

(g) Design of Experiment

Configuration / Reaction Characterization	Engine	Cargo solution			Other reactant		Quenching agent	Reaction time (s)
		Catalyst (Loading)	Reactant	Solvent	Reactant	Solvent		
Kinetic Study	$[bmim]PF_6$	DMAP (0.5 mol%)	menthol, Et_3N	toluene	Ac_2O	toluene	$NaHCO_3$	10 , 20 , 30 , 40, 50, 60, 70, 80, 90
Solvent Screening	$[bmim]PF_6$	DMAP (0.5 mol %)	menthol, Et_3N	toluene, dioxane, DMF, DCE	Ac_2O	toluene, dioxane, DMF, DCE	$NaHCO_3$	30
Optimize Catalyst Loading	$[bmim]PF_6$	0.1 %, 0.5 1.0 1.5 mol %	menthol, Et_3N	toluene	Ac_2O	toluene	$NaHCO_3$	30
Parallel esterification reactions	$[bmim]PF_6$	DMAP (0.5 mol %)	menthol, benzyl alcohol, phenol, Et_3N	toluene	Ac_2O	toluene	$NaHCO_3$	30

Fig. 5 (a-f) Sequential snap shots illustrating the steps of esterification on an EWOD device. (a) An engine-and cargo compound droplet is dispensed from the reservoir. (b) The other reagent solution is dispensed and merged with the engine-and-cargo droplet. (c) Esterification proceeds. (d) A quenching agent is dispensed from the reservoir and transferred to the reacting droplet. (e) As the quenching agent droplet and the reacting droplet merge, reaction is quenched and stops. (f) After quenching, the reaction mixture is drawn out using a syringe and is diluted with DCM within the GC vials. The diluted sample is placed in the GC-MS machine. (g) Design of experiment summarizes conditions of all reactions tested in this study.

4. Result and Discussion

4.1 Qualification of an engine-and-cargo system

According to Ren et al.[42], most of chemical and biological applications of lab-on-chip devices require the volume inconsistency below $\pm$ 5 %. To assess the cargo volume inconsistency, we generated 26 engine-and-cargo droplets consecutively and characterized cargo volumes. During the tests, the cargo reservoir was kept refilled as it depleted. As it is evident from Fig. 6(a), after 3 dispensing of droplets with the average volume (black dots), the fourth droplet (red dots) was dispensed with larger volume than the average. The standard deviation of droplet volume was $\pm$ 13%. This is attributed to volume changes of the reservoir puddle after several dispensing of engine-and-cargo droplets. Guan et al.[43] reported that in an EWOD device a volume of a dispensed droplet has the dependency on a volume of the reservoir puddle. Based on this result, we carefully maintained the cargo reservoir filled properly during all reaction tests. Moreover, droplets with the larger cargo volume than the average were discarded before it proceeded to the reaction. As shown in the insets of Fig. 6(a), the cargo area difference in average droplets and discarded ones was visibly noticeable and easy to screen. With visual screening, we could maintain the volume inconsistency of cargo as low as $\pm$ 3 % throughout all tests.

The engine fluid is not a reagent for esterification while it stays in the reacting droplet during the course of the reaction. It needs to be established that the presence of engine fluid would not interfere the reaction. Moreover, in this study, adding color dye to the engine fluid is desirable for clear visualization of experiments. To identify reaction compatibility of the engine and color dye, we briefly investigated three off-chip reactions; (1) the model esterification, (2) the esterification in the presence the ionic liquid, and (3) the esterification in the presence of ionic liquid and the green food dye. As shown in Fig. 6(b) and (c), all three reactions showed full conversions and provided the ester product cleanly. Conditions for GC-MS spectrometry analysis can be found in ESI.

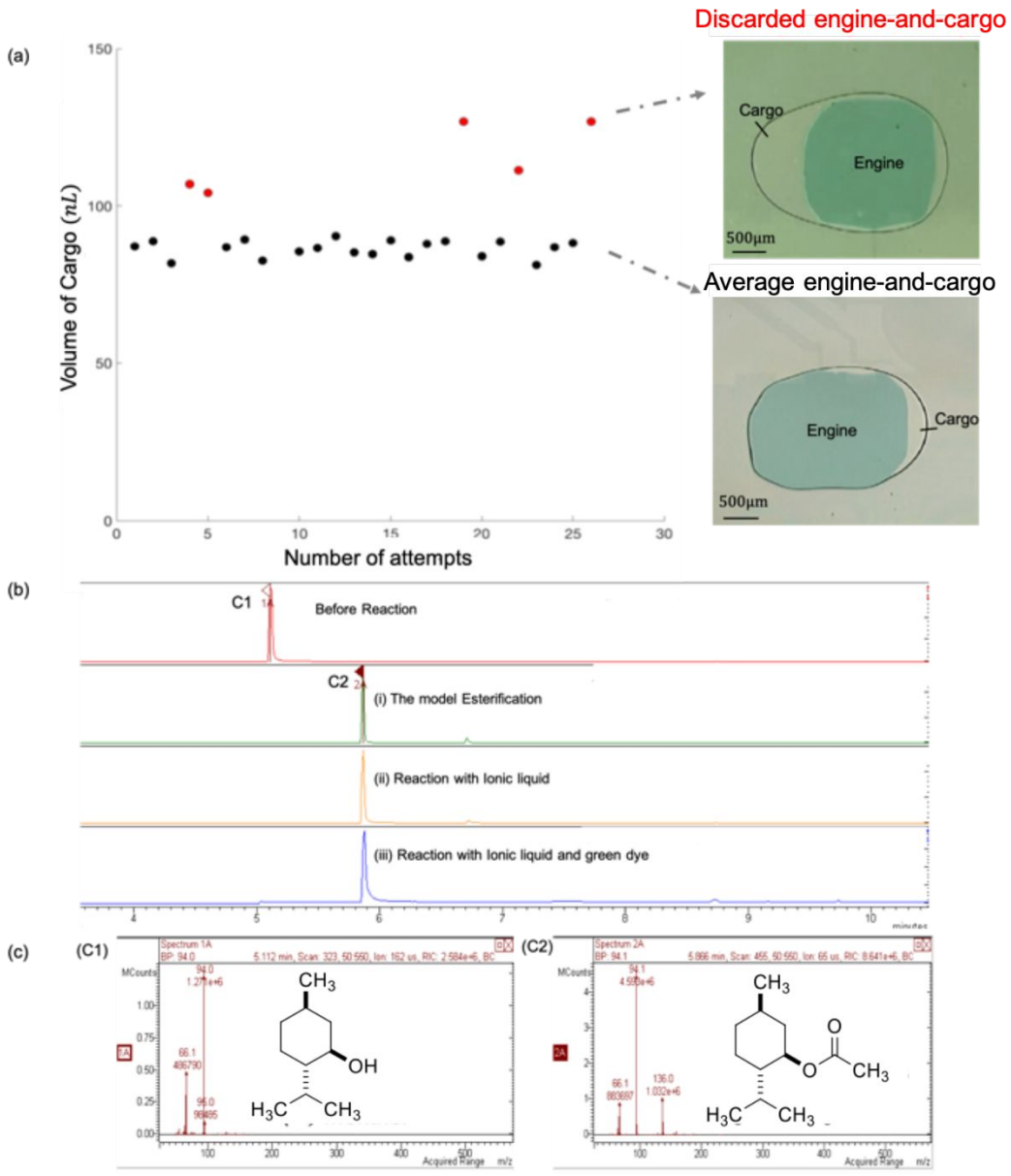

Fig. 6 (a) The cargo volume of 26 engine-and-cargo droplets consecutively dispensed from a reservoir. Inset photos are screenshots of engine-and-cargo droplets during tests. Droplet with larger cargo volume than average were visibly noticeable and were discarded before reaction tests. (b) GC spectrometry results of 3 off-chip reactions. All three reactions showed full conversions and provided the ester product cleanly. (c) MS results confirm the identity of menthol (e.g., C1) before the reaction and acetylated menthol (e.g., C2) after all three experiments.

4.2 Optimization of the reaction

Reaction conditions often need to be optimized to achieve efficient reactions. Typically, optimized reaction conditions can be determined by conversion data from a number of reactions with varying reaction parameters.[44-46] Unquestionably, such reaction optimization is a tedious process that requires substantial resources including time and efforts, and it generates chemical wastes. An EWOD digital microfluidic technology is particularly useful to address this issue; an EWOD device can readily provide arrays of droplets and each droplet carries unique reaction conditions while they are individually controlled.[47] These features make an EWOD device suitable for the high-throughput (in numbers, not in volume) screening platform. In this study, we performed total 60 on-chip tests (3 tests per each of 20 different reaction conditions) and the conversion data from these tests were used to optimize the esterification reaction as followed.

4.2.1 Kinetics study

Study of reaction kinetics is an essential part of the reaction optimization because it provides insights into the reaction mechanism.[48, 49] Kinetics study typically associates with a quenching process in which a quenching agent is added to the reaction mixture to stop the reaction at a desired time and conversion measurement is followed. However, quenching a reaction in a macroscale is not a well-controlled process because of the time for applying a quenching agent and its homogeneous diffusion throughout an entire reactor. These factors are, indeed, negligible in microscale reactions due to possible automated fluid handling and the short diffusion length. Consequentially, large numbers of precise conversions data can be obtained quickly and easily in a microscale reaction.

To this end, we quenched reactions at 9 different times (i.e., 10 – 90 s at 10 s interval). Figure 7 presents kinetic data of same reactions of lab scale (i.e. NMR) tests and on-chip tests. Procedure for lab-scale reactions and the NMR study details can be found in ESI. As shown, the conversion from reactants to the product increased as the reaction proceeds in both lab-scale and on-chip reactions. This confirms that an EWOD chip is capable to carry out accurate quenching of reactions and to provide quick and easy kinetic data. A notable difference between on-chip and off-chip reactions was reaction kinetics; substantially improved kinetics of the on-chip reactions was

observed. For example, while the lab-scale reaction reached to 90% conversion in 30 min, the on-chip reaction reached to 97 % conversion only in 90 s. This result agrees very well with the reports of esterification reactions in microchannel.[36-39] Standard deviation of conversion percent at each quenching time was evaluated (error bars on all on-chip data points and selected lab-scale data points). As shown, standard deviation of on-chip and lab scales ranged very similar (~ $\pm$ 3 %) even though on-chip quenching was done with much short time interval, thus more challenging. Standard deviations of on-chip reaction measurement became bit larger in the later time because of possible evaporation of the reaction mixture. Overall, an EWOD microfluidics is a versatile microscale organic chemical reaction platform which can deliver significantly enhanced reaction kinetics with precise reaction control. One can use this technology to determine the order of reactions and the reaction rate constants.

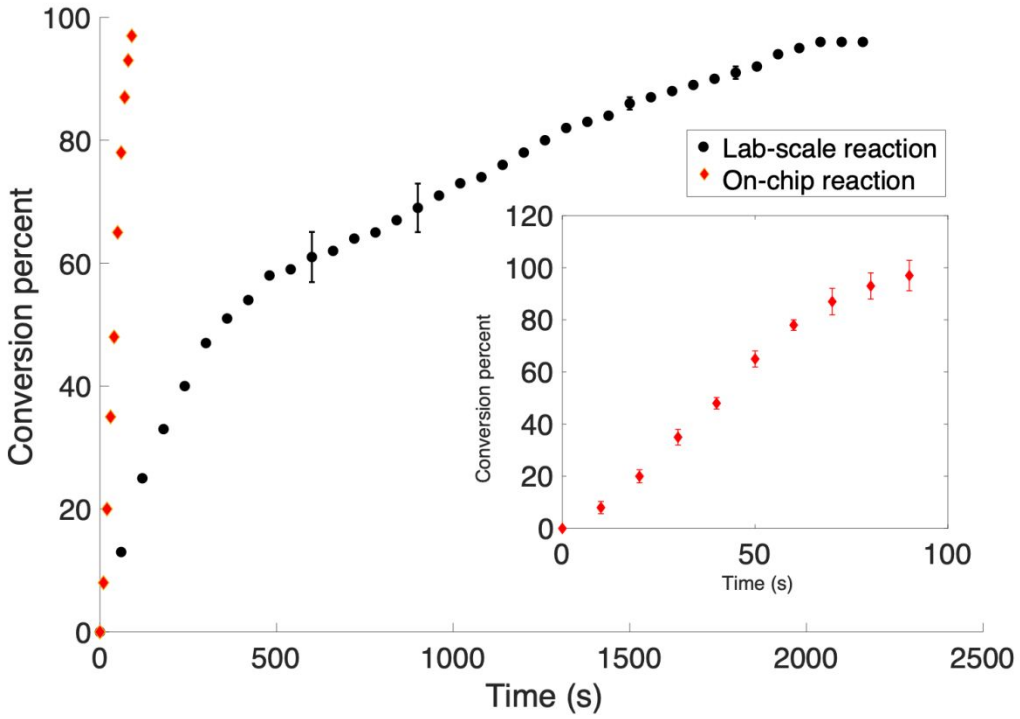

Fig. 7 The conversion percent of lab-scale and on-chip esterification of menthol for different reaction times. For all reactions, toluene was used as solvent and concentration of catalyst (DMAP) was kept at 0.5 mol %. Dots and error bars are the average conversions and standard deviations from 3 reactions per each, respectively.

4.2.2 Solvent Screening

Different solvents were tested to study their impact on esterification reaction. For all tests, catalyst concentration and reaction time were fixed at 0.5 mol % and 30 s, respectively. A conversion rate of esterification of menthol with Ac2O in four different solvents are shown in Fig. 8 where SPI indicates solvent polarity index. Esterification of menthol with less-polar solvents screened in this study [e.g., DCE (SPI, 3.7), dioxane (SPI, 4.8), and toluene (SPI, 2.4)] gave substantially higher conversions, compared with the reaction with polar solvent [e.g., N,N-dimethylformamide (SPI, 6.4)].[50] This result generally agrees with literature precedents which concern flask-based reactions. In both macroscale experiments from literature and the microscale reactions in this study, the SPI values of those less-polar solvents do not proportionally correlated with the order of the reaction efficiency, presumably because other reaction parameters can together impact on the overall efficiency of the reactions.[51]

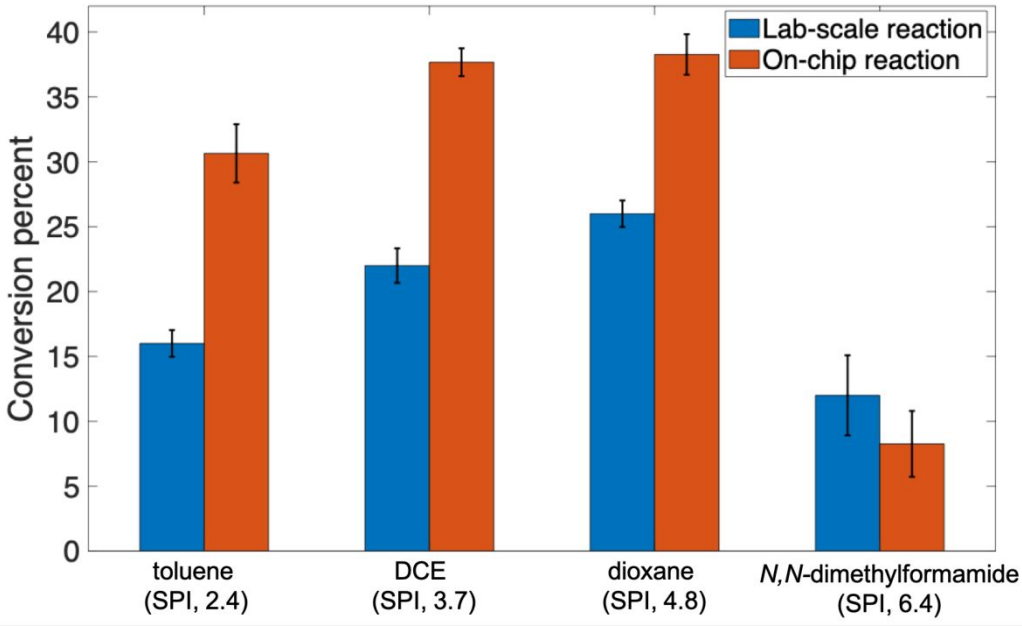

Fig. 8 Conversion of lab-scale and on-chip esterification of menthol in the presence of different solvents including toluene, dioxane, N,N-dimethylformamide, and DCE, at first 30 s. The concentration of catalyst was kept at 0.5 mol % throughout all the solvent screening experiments. Columns and error bars are the average conversions and standard deviations from 3 reactions per each, respectively. Solvent polarity index (SPI) of each solvent is co-labeled.

4.2.3 Catalyst loading optimization

DMAP has been an efficient catalyst for traditional flask-based acylation reactions.[51] In this study, we demonstrated the use of DMAP as a promising catalyst for esterification of the less reactive alcohols (i.e., secondary alcohols) on EWOD microfluidics platform. To investigate the optimal loading of DMAP, four different concentrations (0.1, 0.5, 1.0, and 1.5 mol %) were examined.

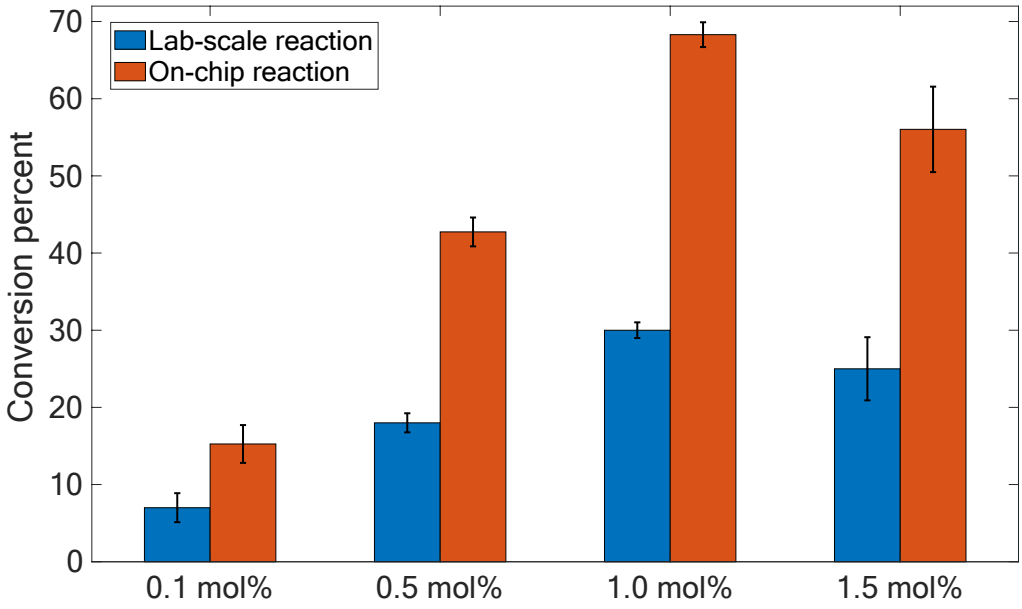

Fig. 9 Conversion of lab-scale and on-chip esterification of menthol with 4 different concentrations of DMAP. For the catalyst loading optimization study, the type of solvent (toluene) and the reaction time (30 s) were fixed for all tests. Columns and error bars are the average conversions and standard deviations from 3 reactions per each, respectively.

As seen from Fig. 9, the higher concentration of DMAP resulted in better yield. However, the loading of 1.5 mol % of DMAP slightly diminished yield. It is likely attributed to solubility of DMAP in toluene, impacting on reaction kinetics. For instance, at the higher concentration of DMAP, pyridinium salt precipitates, which might lead to off-cycle of the catalyst. A similar result was reported by Sakakura et al.[51] in a flask chemistry. Similar to the solvent screening case, on-chip data agrees very well with lab-scale data in this case. Lab-scale reaction shows lower

conversions than on-chip reaction due to its slower kinetics given the reaction time (30 s), yet both tests reach to the same conclusion in optimal concentration of DMAP.

4.3 Parallel esterification reactions

Over the past decades, microscale combinational synthesis has been actively sought.[52-55] Kikutani et al.[56] demonstrated 2×2 combinatorial synthesis of amides through a parallel micro-flow reactor system in a single glass microchip. This approach is mainly based on micro unit operations (MUOs) in pressure driven multi-phase laminar flow networks. Theberge et al.[57] proposed a droplet-based microfluidic platform for combinatorial library synthesis of potential drug candidates, where a 7 × 3 library of potential enzyme inhibitors was used. In both cases the design and architecture of the device are quite complicated. For examples, Kikutani et al.[56] utilized three parallel plates to prevent the cross-contamination that caused the complexity in the fabrication process.

On the other hand, an EWOD digital microfluidic device intrinsically has multiplexing capability so that achieving M × N combinations of reactants can be easily done without any complicate modification of a device. Moreover, each droplet can form an independent microreactor; therefore, cross-contamination and crosstalk can be minimized or eliminated, and reaction conditions constituting each combination of reactants can be individually controlled or altered. As a small step toward the EWOD device for combinatorial syntheses, we performed esterification reactions of three different substrates in a single device. Each droplet was independently generated and manipulated; all other reaction conditions, e.g., solvent, catalyst concentration, and reaction time, were predetermined (Fig. 5(g)).

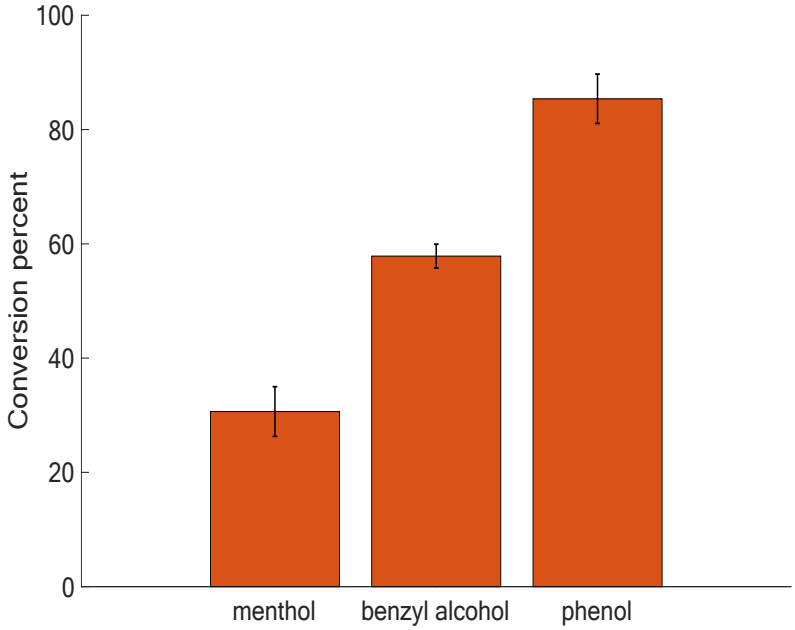

Fig. 10 Conversion of esterification of menthol, benzyl alcohols, and phenol in the presence of toluene, during the first 30 s of on-chip reaction.

As shown in Fig. 10, phenol underwent the esterification in the high yield (85%), compared to benzyl alcohols and menthol in the first 30 s of the reactions. This result is consistent with well-known reactivity of acylation of alcohols and phenols. Structurally, phenol possesses more acidic hydrogen, yet a less nucleophilic oxygen donor than the alcohols. This feature leads to mechanistically different reaction pathways; phenols first undergo facile deprotonation by either DMAP or auxiliary base (e.g., Et_3N) and the resulting oxyanion attacks acylpyridinium ion generated from a reaction of Ac_2O and DMAP.[58, 59] This differs from nucleophilic attack of alcohol to acylpyridinium followed by deprotonation. As expected, sterically less encumbered benzyl alcohol is more reactive toward acylation vis-à-vis menthol.[60, 61] Overall, our result shows that an EWOD device is capable of hosting a library of reagents and permitting combinatorial organic synthesis with organic solvents. Notably, this technology will be a valuable tool for rapidly elucidating of the reactivity difference of reagents or substrates and providing mechanistic insights into a range of organic transformations.

5. Conclusion

This work demonstrated that an EWOD digital microfluidic platform is an alternative or a complementary tool to microreactors based on continuous channel flow for organic synthesis. In this study, we introduced the "engine-and-cargo" strategy that addressed the shortcoming of an EWOD device; the novel technique makes an EWOD device capable of handling electrically non-responsive fluids, particularly organic solvents, where organic fluids are not generally electrically movable. With the engine-and-cargo approach, esterification involving alcohols and phenols with acetic anhydride in the presence of base and DMAP were successfully carried out on EWOD devices. The study on reaction kinetics established benefits from an EWOD device on account of rapid and precise quenching of reactions. Furthermore, rapid reaction optimization was realized on a EWOD device, examining two parameters including solvents and catalyst loading. Finally, we demonstrated the 3×1 combinatorial synthesis of esters with three substrates in a rapid fashion.

Electronic Supplementary Material (ESI)

See supplementary material for EWOD device fabrication, Lab scale reactions and the NMR study details, Mass Spectroscopy (GC-MS), Image-based volume measurement and the experimental video of esterification of menthol on an EWOD device.

Acknowledgement

This study was supported by National Science Foundation (NSF) (Grant No. ECCS-1254602) and UTA Interdisciplinary Research Program (IRP).

Conflicts of Interests

There are no conflicts to declare.

References

1. M. M. Singh, Z. Szafran and R. M. Pike, *Journal of Chemical Education*, 1999, **76**, 1684.
2. Z. Szafran, M. M. Singh and R. M. Pike, *Journal of Chemical Education*, 1989, **66**, A263.
3. N. Kockmann, M. Gottsponer, B. Zimmermann and D. M. Roberge, *Chemistry–A European Journal*, 2008, **14**, 7470-7477.
4. K. S. Elvira, X. C. i Solvas, R. C. Wootton and A. J. Demello, *Nature chemistry*, 2013, **5**, 905.
5. S. H. DeWitt, *Current Opinion in Chemical Biology*, 1999, **3**, 350-356.
6. P. L. Mills, D. J. Quiram and J. F. Ryley, *Chemical Engineering Science*, 2007, **62**, 6992-7010.
7. P. Löb, H. Löwe and V. Hessel, *Journal of Fluorine Chemistry*, 2004, **125**, 1677-1694.
8. P. W. Miller, N. J. Long, A. J. de Mello, R. Vilar, J. Passchier and A. Gee, *Chemical communications*, 2006, 546-548.
9. G. M. Greenway, S. J. Haswell, D. O. Morgan, V. Skelton and P. Styring, *Sensors and Actuators B: Chemical*, 2000, **63**, 153-158.
10. V. Skelton, G. M. Greenway, S. J. Haswell, P. Styring, D. O. Morgan, B. Warrington and S. Y. Wong, *Analyst*, 2001, **126**, 7-10.
11. P. Watts and S. J. Haswell, *Chemical Society Reviews*, 2005, **34**, 235-246.
12. L. Kang, B. G. Chung, R. Langer and A. Khademhosseini, *Drug discovery today*, 2008, **13**, 1-13.
13. A. A. Mariod and H. Fadul, *Acta Scientiarum Polonorum Technologia Alimentaria*, 2013, **12**, 135-147.
14. K. Choi, A. H. Ng, R. Fobel and A. R. Wheeler, *Annual review of analytical chemistry*, 2012, **5**, 413-440.
15. S. K. Cho, H. Moon and C.-J. Kim, *Journal of Microelectromechanical systems*, 2003, **12**, 70-80.
16. P. Dubois, G. Marchand, Y. Fouillet, J. Berthier, T. Douki, F. Hassine, S. Gmouh and M. Vaultier, *Analytical chemistry*, 2006, **78**, 4909-4917.
17. P. Y. Keng, S. Chen, H. Ding, S. Sadeghi, G. J. Shah, A. Dooraghi, M. E. Phelps, N. Satyamurthy, A. F. Chatziioannou and R. M. van Dam, *Proceedings of the National Academy of Sciences*, 2012, **109**, 690-695.
18. M. J. Jebrail, A. H. Ng, V. Rai, R. Hili, A. K. Yudin and A. R. Wheeler, *Angewandte Chemie International Edition*, 2010, **49**, 8625-8629.
19. D. Chatterjee, B. Hetayothin, A. R. Wheeler, D. J. King and R. L. Garrell, *Lab on a Chip*, 2006, **6**, 199-206.
20. M. Torabinia, A. Farzbod and H. Moon, *Journal of Applied Physics*, 2018, **123**, 154902.

21. D. Brassard, L. Malic, F. Normandin, M. Tabrizian and T. Veres, *Lab on a Chip*, 2008, **8**, 1342-1349.
22. J. Li, Y. Wang, H. Chen and J. Wan, *Lab on a Chip*, 2014, **14**, 4334-4337.
23. S.-K. Fan, T.-H. Hsieh and D.-Y. Lin, *Lab on a Chip*, 2009, **9**, 1236-1242.
24. M. Brivio, W. Verboom and D. N. Reinhoudt, *Lab on a Chip*, 2006, **6**, 329-344.
25. S. M. George and H. Moon, *Biomicrofluidics*, 2015, **9**, 024116.
26. P. A. Wijethunga, Y. S. Nanayakkara, P. Kunchala, D. W. Armstrong and H. Moon, *Analytical chemistry*, 2011, **83**, 1658-1664.
27. S. Paul and H. Moon, 2017.
28. A. Farzbod and H. Moon, *Biosensors and Bioelectronics*, 2018, **106**, 37-42.
29. N. Phonsatta, P. Deetae, P. Luangpituksa, C. Grajeda-Iglesias, M. C. Figueroa-Espinoza, J. r. m. Le Comte, P. Villeneuve, E. A. Decker, W. Visessanguan and A. Panya, *Journal of agricultural and food chemistry*, 2017, **65**, 7509-7518.
30. B. Pérez, S. Anankanbil and Z. Guo, in *Fatty Acids*, Elsevier, 2017, pp. 329-354.
31. J. Sun, L. Pan, D. C. Tsang, Z. Li, L. Zhu and X. Li, *Environmental Science and Pollution Research*, 2018, **25**, 34-42.
32. J. Bos and T. W. Muir, *Journal of the American Chemical Society*, 2018, **140**, 4757-4760.
33. S. E. Branz, R. G. Miele, R. K. Okuda and D. A. Straus, *Journal of chemical education*, 1995, **72**, 659.
34. M. K. Reilly, R. P. King, A. J. Wagner and S. M. King, *Journal of Chemical Education*, 2014, **91**, 1706-1709.
35. J. W. Swarts, P. Vossenberg, M. H. Meerman, A. E. Janssen and R. M. Boom, *Biotechnology and bioengineering*, 2008, **99**, 855-861.
36. J. Wang, S.-S. Gu, H.-S. Cui, X.-Y. Wu and F.-A. Wu, *Bioresource technology*, 2014, **158**, 39-47.
37. T. Razzaq, T. N. Glasnov and C. O. Kappe, *European Journal of Organic Chemistry*, 2009, **2009**, 1321-1325.
38. M. Brivio, R. E. Oosterbroek, W. Verboom, M. H. Goedbloed, A. van den Berg and D. N. Reinhoudt, *Chemical communications*, 2003, 1924-1925.
39. C. Wiles, P. Watts, S. J. Haswell and E. Pombo-Villar, *Tetrahedron*, 2003, **59**, 10173-10179.
40. Y. Okuno, S. Isomura, A. Sugamata, K. Tamahori, A. Fukuhara, M. Kashiwagi, Y. Kitagawa, E. Kasai and K. Takeda, *ChemSusChem*, 2015, **8**, 3587-3589.
41. M. Torabinia, A. Venkatesan and H. Moon, 2018.
42. H. Ren, R. B. Fair and M. G. Pollack, *Sensors and Actuators B: Chemical*, 2004, **98**, 319-327.
43. Y. Guan, A. Y. Tong, N. J. B. Nikapitiya and H. Moon, *Microfluidics and Nanofluidics*, 2016, **20**, 39.
44. S. W. Krska, D. A. DiRocco, S. D. Dreher and M. Shevlin, *Accounts of chemical research*, 2017, **50**, 2976-2985.

45. A. B. Santanilla, E. L. Regalado, T. Pereira, M. Shevlin, K. Bateman, L.-C. Campeau, J. Schneeweis, S. Berritt, Z.-C. Shi and P. Nantermet, *Science*, 2015, **347**, 49-53.
46. K. D. Collins and F. Glorius, *Accounts of chemical research*, 2015, **48**, 619-627.
47. T. Kaminski and P. Garstecki, *Chemical Society Reviews*, 2017, **46**, 6210-6226.
48. S. J. Klippenstein, V. S. Pande and D. G. Truhlar, *Journal of the American Chemical Society*, 2014, **136**, 528-546.
49. S. Khan, X. He, J. A. Khan, H. M. Khan, D. L. Boccelli and D. D. Dionysiou, *Chemical engineering journal*, 2017, **318**, 135-142.
50. L. Snyder, *Journal of Chromatographic Science*, 1978, **16**, 223-234.
51. A. Sakakura, K. Kawajiri, T. Ohkubo, Y. Kosugi and K. Ishihara, *Journal of the American Chemical Society*, 2007, **129**, 14775-14779.
52. P. M. Valencia, E. M. Pridgen, M. Rhee, R. Langer, O. C. Farokhzad and R. Karnik, *ACS nano*, 2013, **7**, 10671-10680.
53. X. Zhang and Y. Xiang, *Journal of Materiomics*, 2017, **3**, 209-220.
54. V. Nittis, R. Fortt, C. Legge and A. De Mello, *Lab on a Chip*, 2001, **1**, 148-152.
55. M. C. Mitchell, V. Spikmans, A. Manz and A. J. de Mello, *Journal of the Chemical Society, Perkin Transactions 1*, 2001, 514-518.
56. Y. Kikutani, T. Horiuchi, K. Uchiyama, H. Hisamoto, M. Tokeshi and T. Kitamori, *Lab on a Chip*, 2002, **2**, 188-192.
57. A. B. Theberge, E. Mayot, A. El Harrak, F. Kleinschmidt, W. T. Huck and A. D. Griffiths, *Lab on a Chip*, 2012, **12**, 1320-1326.
58. S. Xu, I. Held, B. Kempf, H. Mayr, W. Steglich and H. Zipse, *Chemistry–A European Journal*, 2005, **11**, 4751-4757.
59. A. C. Spivey and S. Arseniyadis, *Angewandte Chemie International Edition*, 2004, **43**, 5436-5441.
60. P. Lucio Anelli, C. Biffi, F. Montanari and S. Quici, *The Journal of Organic Chemistry*, 1987, **52**, 2559-2562.
61. D. B. Dess and J. Martin, *Journal of the American Chemical Society*, 1991, **113**, 7277-7287.

On-chip organic synthesis enabled by engine-and-cargo in an electrowetting-on-dielectric digital microfluidic device